Practical theory of the multilayered transition radiation detector*

X. Artru
CERN, Geneva, Switzerland

G. B. Yodh
Department of Physics and Astronomy, University of Maryland, College Park, Maryland 20742

G. Mennessier
Laboratoire de Physique Theorique et Hautes Energies,† Université de Paris-Sud, Orsay, France

(Received 7 April 1975)

The transition radiation detector for ultrarelativistic particles with a multifoil radiator is studied in the following aspects: x-ray spectrum, γ dependence, interference effects, saturation at high γ, effects of irregularities, and multiple scattering. The analysis is simplified by reducing the various parameters to essentially three dimensionless quantities: a scaled Lorentz factor Γ, a scaled frequency ν, and the ratio $\tau =$ foil spacing/foil thickness. Large threshold effects due to interference are predicted which can be used to build a threshold detector or to measure the x-ray index of refraction of a material. Theoretical curves are given. Photon statistics, optimization of the detector, and computational method are discussed briefly.

I. INTRODUCTION

Transition radiation is the electromagnetic radiation that is emitted when a charged particle traverses the boundary between two media of different dielectric or magnetic properties.[1] Like Čerenkov emission, this process depends on the velocity of the particle and is a collective response of the matter surrounding the trajectory. Like bremsstrahlung, it is sharply peaked in the forward direction if the particle is ultrarelativistic. In this case, the major part of the radiated energy is in x rays. The mean number of photons per transition is small, of the order of the fine structure constant α. But its sizeable γ dependence ($\gamma = E/m$ is the Lorentz factor of the radiating particle) provides a widely discussed possibility of designing a very high energy particle detector which could distinguish particles of different masses at a given momentum, or which could measure the energy of particles of known mass when conventional detectors become inoperative (e.g., at $\gamma \gtrsim 1000$).

The main object of this paper is to provide a concise general formulation of the theoretically predicted yields from a stack of foils, which can be useful for the design of practical detectors, and to clarify the vast amount of theoretical discussion found in the literature.[2-4] We write it as "self contained" as possible. Special emphasis is put on the interference effects, which can enhance the γ dependence. In particular, we stress the importance of the thresholds, i.e., sudden jumps in the curve for energy radiated versus γ. These thresholds may be used for a threshold detector, but, anyway, cannot be ignored and are interesting theoretically.

These thresholds could provide a determination of the plasma frequency of the radiator material. Also important are the saturation limits at very high energy, which are due to the "formation-zone" effect and to the nonzero gas density between the foils.

In Sec. II, we give the theoretical formulas for transition radiation in the x-ray region from a single surface, a single foil, and a stack of N foils. These include absorption effects in the foil and gaps.

In Sec. III, we give the qualitative features of the yield integrated over angles in terms of the two dimensionless variables ν and Γ and the parameter τ. For nonvacuum gaps, we give a simple transformation on the quantities γ and ω_{plasma} which allows us to use the same yield function as in the vacuum case.

II. GENERAL THEORETICAL FORMULA OF THE DIFFERENTIAL YIELD

A. Transition radiation at the boundary of two semi-infinite media

When a charged particle passes the boundary between two media of different dielectric or magnetic properties, radiation is emitted because the Coulomb field of the particle has to readjust itself.[5]

Let $\{\vec{E}_1(\vec{r}, t), \vec{H}_1(\vec{r}, t)\}$ be the equilibrium solution of the inhomogeneous Maxwell equations in medium 1, i.e., the Lorentz-transformed Coulomb field of the particle, and $\{\vec{E}_2, \vec{H}_2\}$ the same in medium 2. $\{\vec{E}_1, \vec{H}_1\}$ and $\{\vec{E}_2, \vec{H}_2\}$ do not match at the boundary. In order to satisfy the continuity equations, we must add, in each medium, respectively, a solu-

tion of the homogeneous Maxwell equations. This one is transition radiation. Let us denote it by $\{\vec{E}_R, \vec{H}_R\}$. With the Poynting vector we get the differential energy flux. The complete expression is rather complicated. But at high γ, most of the energy is in x rays, and primarily emitted in the forward direction. For these x rays, the material medium can be considered as an electron gas, with a dielectric "constant" given by

$$\epsilon(\omega) = 1 - \omega_P^2/\omega^2 = 1 - \xi^2 , \tag{2.1}$$

where ω_P is the plasma frequency of the medium[6]:

$$\omega_P^2 = 4\pi\alpha n_e/m_e \tag{2.2}$$

(n_e = electron density, $\alpha = \frac{1}{137}$). A partial density ρ of an element ${}_ZX^A$ gives the contribution

$$\omega_P^2 = 4\pi\alpha ZA^{-1}\mathfrak{N}\rho/m_e \quad (\mathfrak{N} = \text{Avogadro number})$$
$$\simeq 2(Z/A)(\rho/\text{g cm}^{-3})(21\text{ eV})^2 . \tag{2.2'}$$

ω is of the order of $\gamma\omega_P$. Thus, under the conditions

$$\gamma \gg 1 ; \quad \xi_1^2, \xi_2^2 \ll 1 ; \quad \theta \ll 1$$

(θ is the angle between the particle trajectory and the direction of observation), the energy radiated per unit solid angle, per unit frequency interval can be approximated by[5]

$$\frac{d^2W}{d\omega\, d\Omega} = \frac{\alpha}{\pi^2}\left|\frac{\theta}{\gamma^{-2}+\theta^2+\xi_1^2} - \frac{\theta}{\gamma^{-2}+\theta^2+\xi_2^2}\right|^2 . \tag{2.3}$$

We see from this expression that the radiation is concentrated in a narrow cone, θ^2 being of an order ranging from $\gamma^{-2}+\xi_1^2$ to $\gamma^{-2}+\xi_2^2$. As long as this cone is completely contained in the second medium, there is no dependence on the angle of incidence of the particle relative to the boundary (Fig. 1).

B. Transition radiation emitted during the passage through layers of different media

Let us consider the case of n parallel surfaces separating $n+1$ different media (Fig. 2). We label the surfaces $1, 2, \ldots, n$ and the media $0, 1, \ldots, n$. Using the same method as for one single boundary, we can say that the electromagnetic field in medium i is the sum of $\{\vec{E}_i, \vec{H}_i\}$ (solution of the inhomogeneous Maxwell equations) and the $\{\vec{E}_R^j, \vec{H}_R^j\}$'s necessary to match the fields at the different boundaries. $\{\vec{E}_R^j, \vec{H}_R^j\}$ is the radiation field that would be emitted by the jth interface alone, modified, however, by all possible refractions and reflections on the n boundaries, and also by the absorption in the media.

In our case ($\omega \gg \omega_P$, $\gamma \gg 1$) we can neglect (i) backward emission, (ii) reflections on the boundaries, and (iii) change in θ because of the refractions. Therefore, the amplitude of the radiation which emerges from the last boundary is proportional to

$$\vec{E}(\omega, \vec{\theta}) = \sum_{j=1}^{n} \vec{e}^{\,j}(\omega, \vec{\theta}) \exp\left(-\sum_{m \geq j} \sigma_m + i\varphi_m\right) . \tag{2.4}$$

$\vec{e}^{\,j}$ is the single-surface amplitude. $\vec{\theta}$, of length θ, is the difference between the unit vectors representing the photon and particle directions. Up to a numerical factor

$$\vec{e}^{\,j}(\omega, \vec{\theta}) = \frac{\vec{\theta}}{\gamma^{-2}+\theta^2+\xi_{j-1}^2} - \frac{\vec{\theta}}{\gamma^{-2}+\theta^2+\xi_j^2} , \tag{2.5}$$

$e^{-\sigma_m}$ is the absorption factor in the mth layer and φ_m the phase retardation due to the difference of speeds of the particle and the wave in this layer:

$$\varphi_m = \omega l_m/v - \vec{k}\cdot\vec{l}_m , \tag{2.6}$$

where $\vec{k}_m$ is the wave vector in medium m and $\vec{l}_m$ the particle path in this layer. Using

$$k_m = \sqrt{\epsilon_m}\,\omega \simeq (1 - \tfrac{1}{2}\xi_m^2)\omega , \tag{2.7}$$

$$1/v \simeq 1 + \gamma^{-2}/2 , \tag{2.8}$$

$$\vec{k}_m\cdot\vec{l}_m \simeq k_m l_m \cos\theta \simeq k_m l_m(1 - \tfrac{1}{2}\theta^2) , \tag{2.9}$$

we get

$$\varphi_m \simeq (\gamma^{-2} + \theta^2 + \xi_m^2)\omega l_m/2 . \tag{2.10}$$

In writing (2.9), we have assumed that all the $\vec{l}_m$'s are collinear, i.e., we neglect possible multiple scattering of the particle. It will be useful to consider φ_m as the sum of a "space term"

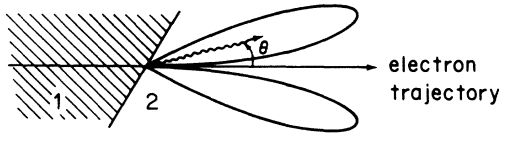

FIG. 1. Angular distribution of the single-surface intensity.

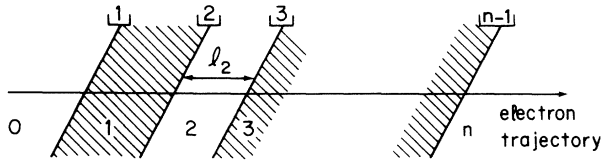

FIG. 2. n-interface radiator.

$$(\gamma^{-2}+\theta^2)\omega l_m/2 \tag{2.11}$$

and a "mass term" proportional to the mass thickness [see Eq. (2.2′)],

$$l_m\omega_{P_m}{}^2/2\omega, \tag{2.12}$$

which vary inversely with ω.

Let us introduce the "formation length"

$$z_m(\theta)=(\gamma^{-2}+\theta^2+\xi_m{}^2)^{-1}2/\omega. \tag{2.13}$$

If $l_m \ll z_m(\theta)$, the two boundaries of the mth medium interfere in such a way that we can ignore the mth layer. This will be called the "formation-zone effect."

Application (a): Yield from one foil in a gas

Here $\xi_0=\xi_2$ and $\vec{e}^1(\omega)=-\vec{e}^2(\omega)$. Whence (neglecting absorption)

$$\left(\frac{d^2W}{d\omega\,d\Omega}\right)_{\text{single foil}} = \left(\frac{d^2W}{d\omega\,d\Omega}\right)_{\text{single surface}} \times 4\sin^2(\varphi_1/2). \tag{2.14}$$

Application (b): Yield from a stack of N foils of constant thickness and spacing

Grouping first the amplitude 2 by 2 in foil amplitudes and then adding coherently these N amplitudes, we get

$$\left(\frac{d^2W}{d\omega\,d\Omega}\right)_{N\text{ foil}} = \left(\frac{d^2W}{d\omega\,d\Omega}\right)_{\text{single foil}} \times I^{(N)}, \tag{2.15}$$

$I^{(N)}$ being the N-foil interference factor given by

$$I^{(N)}=\left|\frac{1-C^N}{1-C}\right|^2, \tag{2.16}$$

$$C=\exp(i\varphi_1+i\varphi_2-\tfrac{1}{2}\sigma_1-\tfrac{1}{2}\sigma_2). \tag{2.17}$$

$I^{(N)}$ depends on θ through φ_1 and φ_2. Introducing the total phase shift of one foil + one gap,

$$\varphi_{12}(\theta^2)\equiv\varphi_1+\varphi_2=(l_1+l_2)(\gamma^{-2}+\theta^2)\omega/2 + (l_1\omega_{P_1}{}^2+l_2\omega_{P_2}{}^2)/2\omega, \tag{2.18}$$

and $\sigma=\sigma_1+\sigma_2$, the absorption in one foil + one gap, we can also write

$$I^{(N)}\equiv I^{(N)}(\varphi_{12},\sigma) = \exp\left(\frac{1-N}{2}\sigma\right)\frac{\sin^2(N\varphi_{12}/2)+\sinh^2(N\sigma/4)}{\sin^2(\varphi_{12}/2)+\sinh^2(\sigma/4)}. \tag{2.19}$$

III. PRACTICAL QUALITATIVE STUDY OF THE YIELD INTEGRATED OVER ANGLE

Preliminary remarks

Although it is possible to measure not only the photon energy but also θ—which is very small in our case of interest—we shall study here only the flux integrated over angles, which is much easier to measure (thus losing some information).

An interesting feature of the γ dependence of $dW/d\omega$ is that it is always increasing with γ: Introducing $x=\gamma^{-2}+\theta^2$, we have

$$\frac{dW}{d\omega}=\frac{\alpha}{\pi}\int_{\gamma^{-2}}^{\infty}\frac{x-\gamma^{-2}}{(x+\xi_1{}^2)^2(x+\xi_2{}^2)^2}dx(\xi_1{}^2-\xi_2{}^2) \times(\text{interference factors}). \tag{3.1}$$

The interference factors are functions of x only (not of γ and θ separately) and are positive. The above formula then clearly defines a monotonic function of γ. If one of the media is vacuum, $dW/d\omega$ increases logarithmically with γ when $\gamma \to \infty$. If ω_{P1} and $\omega_{P2}\neq 0$, $dW/d\omega$ reaches a finite limit when $\gamma\to\infty$ (saturation).

In fact, in the general formulas for the yield, (2.4), (2.5), and (2.10), γ and the two plasma frequencies appear only in the combinations $\gamma^{-2}+\xi_1{}^2$ and $\gamma^{-2}+\xi_2{}^2$. Thus, we have the same yield with the parameters ω_{P1}, ω_{P2}, γ as with vacuum and the parameters

$$\omega'_{P1}=(\omega_{P1}{}^2-\omega_{P2}{}^2)^{1/2}, \quad \omega'_{P2}=0 \text{ (vacuum)} \tag{3.2}$$

and

$$\gamma'=(\gamma^{-2}+\omega_{P2}{}^2/\omega^2)^{-1/2}. \tag{3.3}$$

We always have $\gamma'<\gamma$ and $\omega'_{P1}<\omega_{P1}$; the yield in gas is therefore expected to be smaller than the yield in vacuum. More generally, we conjecture from (3.1)

$$\frac{dW}{d\omega}=\text{decreasing function of } \omega_{P2}. \tag{3.4}$$

The interference factors could overcompensate the decrease of the single-surface integrand but this circumstance will be shown to be unlikely. Anyway, for $\omega_{P2}\neq 0$, the yield saturates when

$$\gamma\gtrsim\gamma'_\infty=\xi_2^{-1}=\omega/\omega_{P2}. \tag{3.5}$$

In normal air ($\omega_{P2}=0.7$ eV) $\gamma'_\infty\sim 10^4$ for 10 keV x rays.

Let us now examine in detail the four cases A. one single boundary, B. one single foil, C. one single gap, and D. a stack of foils regularly spaced.

A. The "single-surface" yield

Integrating (2.3) over Ω, we get

$$\left(\frac{dW}{d\omega}\right)_{\text{single surface}} = \frac{\alpha}{\pi}\left(\frac{\xi_1^2+\xi_2^2+2\gamma^{-2}}{\xi_1^2-\xi_2^2}\ln\frac{\gamma^{-2}+\xi_1^2}{\gamma^{-2}+\xi_2^2}-2\right), \tag{3.6}$$

which depends only on γ/ω. Let us introduce

$$\eta = \omega/\gamma\omega_{P1}, \tag{3.7}$$

$$r = \omega_{P2}^2/\omega_{P1}^2 \quad (\simeq\rho_2/\rho_1). \tag{3.8}$$

As a function of γ we can distinguish three regimes (assuming $r \ll 1$, for instance, a dense material and a gas):

(i) $\gamma \ll \omega/\omega_{P1}$, i.e., $\eta \gg 1$, a very low yield

$$dW/d\omega \simeq \alpha/6\pi\eta^4; \tag{3.9}$$

(ii) $\omega/\omega_{P1} \ll \gamma \ll \omega/\omega_{P2}$, the yield increases logarithmically with γ

$$dW/d\omega \simeq (\ln\eta^{-1}-1)2\alpha/\pi; \tag{3.10}$$

(iii) $\gamma \gg \omega/\omega_{P2} = \gamma'_\infty$, i.e., $\eta \ll r^{1/2}$, the yield is almost constant (saturation). In the general case, the yield is a function of

$$\eta' = \omega/\gamma'\omega'_{P1} = (\eta^2+r)^{1/2}(1-r)^{-1/2}, \tag{3.11}$$

$$\left(\frac{dW}{d\omega}\right)_{\text{single surface}} = \frac{\alpha}{\pi}[(1+2\eta'^2)\ln(1+\eta'^{-2})-2]$$

$$\equiv \frac{\alpha}{\pi}G_{\text{inco}}(\eta'). \tag{3.12}$$

The function $G_{\text{inco}}(\eta)$ is plotted in Fig. 3. In the following, r will be assumed to be small.

Case (i) results in a frequency cutoff, whence the necessary condition for having enough yield

$$\omega \lesssim \gamma\omega_{P1}. \tag{3.13}$$

Integrating over the spectrum, we get the mean energy radiated in one medium vacuum transition[7]

$$W = 2\alpha\gamma\omega_p/3. \tag{3.14}$$

This linear response in γ corresponds to an ideal situation which is unfortunately not met by practical detectors, as we shall see below.

The mean number of photons $\int dW/\omega$, proportional to the area under the curve in Fig. 3, diverges in the soft x-ray region. But we have always some low-energy cutoff. The result is of the order of α, for instance,

$$\text{No. of photons } (\omega > 0.15\gamma\omega_p) \simeq 0.5\alpha, \tag{3.15}$$

whence the necessity of having a large number of foils.

B. The single-foil yield

Here we have to weight formula (3.1) by the interference factor

$$4\sin^2(\varphi_1/2) = 4\sin^2[(\gamma^{-2}+\theta^2+\xi_1^2)\omega l_1/4]. \tag{3.16}$$

By the way, let us remark that the integrand in (3.1) is a decreasing function of ξ_2^2. This proves (3.4) for the single-foil case.

i. The formation-zone effect

In the relevant region of integration over θ, φ_1 is of the order of $\omega l_1(\gamma^{-2}+\xi_1^2)/2$. Therefore, if the thickness is much less than the quantity

$$Z_1 = (\gamma^{-2}+\xi_1^2)^{-1}2/\omega = z_1(\theta=0), \tag{3.17}$$

which is referred to as the "formation zone," the yield is strongly reduced by the interference effect (it varies as φ_1^2). The formation zone can also be understood as the minimum distance in-

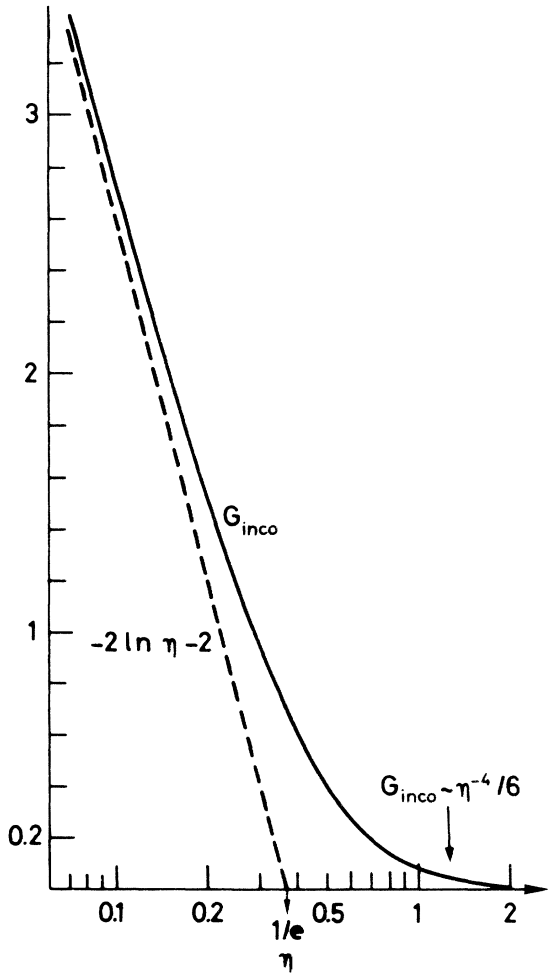

FIG. 3. The single-surface yield in the vacuum case.

side the foil required for the electromagnetic field of the particle to reach its new equilibrium configuration. From another point of view, transition radiation is a macroscopic process, so that the radiation yield tends to zero when the foil gets more and more thin. The region of the (ω,γ) plane where the formation-zone effect occurs is shown in Fig. 4. For γ greater than the quantity

$$\gamma_1 = l_1\omega_{P1}/2\,, \tag{3.18}$$

the frequency cutoff, instead of being $\gamma\omega_{P1}$, as in the single-surface case, is rather determined by the formation-zone effect:

$$\varphi_1 \sim \omega l_1 \xi_1^{\,2}/2 = l_1\omega_{P1}^{\,2}/2\omega \sim 1\,. \tag{3.19}$$

The new condition to have enough yield is now

$$\omega < \min(\gamma\omega_{P1}, \omega_1)\,, \tag{3.20}$$

where

$$\omega_1 = l_1\omega_{P1}^{\,2}/2 = \gamma_1\omega_{P1}\,. \tag{3.21}$$

An important consequence is that, for $\gamma > \gamma_1$ and vacuum, the mean radiated energy W ceases to increase linearly with γ but only logarithmically. The coefficient of the logarithm is of the order of $\alpha\omega_1$.

For practical calculations, we have

$$\gamma_1 = 2.5(\omega_{P1}/\mathrm{eV})(l_1/\mathrm{micron}) \tag{3.18'}$$

and roughly

$$(\omega_1/\mathrm{keV}) \simeq 10^4(\rho_1 l_1/\mathrm{g\,cm^{-2}})\,. \tag{3.21'}$$

For a given x-ray detector, the condition (3.20) implies a minimum surface density for the foil which is independent of the material. Let $\bar{\omega}$ be the mean detected frequency and let us require (for reasons which will be explained below) $\omega_1 \sim 3\bar{\omega}$. Then

$$(\rho_1 l_1/\mathrm{g\,cm^{-2}}) \sim 3\times 10^{-4}(\bar{\omega}/\mathrm{keV})\,. \tag{3.22}$$

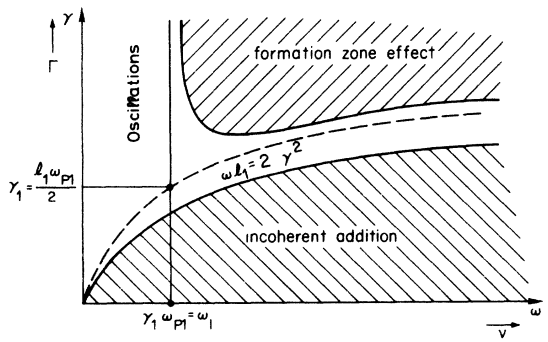

FIG. 4. Different regions of the ω, γ plane relevant for the single-foil yield (in the vacuum case).

Experimentally, the formation-zone effect has been observed by reducing the foil thickness to a few microns.[8]

2. *Introduction of scaled variables*

For reasons which are apparent in Fig. 4, it is convenient to replace γ and ω by the dimensionless quantities

$$\Gamma = \gamma/\gamma_1\,, \tag{3.23}$$

$$\nu = \omega/\omega_1\,, \tag{3.24}$$

with γ_1 and ω_1 defined by (3.18) and (3.21).

In terms of these new quantities, the intensity is given by

$$\left(\frac{dW}{d\omega}\right)_{\text{single foil}} = \frac{2\alpha}{\pi}\int_a^\infty (y-a)dy\left(\frac{1}{y}-\frac{1}{y+V}\right)^2 2\sin^2\frac{y+V}{2} \equiv \frac{2\alpha}{\pi}G\,, \tag{3.25}$$

where

$$a = \nu\Gamma^{-2} + \gamma\nu^{-1} = l_1/Z_2\,, \tag{3.26}$$

Z_2 being the formation zone in the external medium

$$Z_2 = 2(\gamma^{-2} + \xi_2^{\,2})^{-1}/\omega\,, \tag{3.27}$$

and

$$V = (1-\gamma)\nu^{-1} = l_1/Z_1 - l_2/Z_2\,. \tag{3.28}$$

The integration variable y is now

$$y = \varphi_1(\theta^2) - V = (\gamma^{-2} + \theta^2 + \xi_2^{\,2})\omega l_1/2\,. \tag{3.29}$$

The yields from different kinds of foils are all given by a "universal" function of a and V. In the case of vacuum gaps, we have

$$\left.\begin{aligned} a &= \nu\Gamma^{-2} \\ V &= \nu^{-1} \end{aligned}\right\}\text{(vacuum gaps)}, \tag{3.30}$$

and it is more convenient to use ν and Γ instead of a and V as arguments of G:

$$G_{\text{vac}} \equiv G(\nu,\Gamma)\,. \tag{3.31}$$

For a foil in gas, if we transform the quantities γ, ω_{P1}, ω_{P2} according to the formulas (3.2) and (3.3), we are left with the vacuum case. Thus

$$G_{\text{gas}} = G(\nu',\Gamma')\,, \tag{3.32}$$

with

$$\nu' = \nu(1-\gamma)^{-1}\,, \tag{3.33}$$

$$\Gamma' = (\Gamma^{-2} + \gamma\nu^{-2})^{-1/2}(1-\gamma)^{-1/2}\,. \tag{3.34}$$

The universal function $G(\nu,\Gamma)$ given by (3.25) and (3.30) is plotted in Fig. 5 for the range of interest. An expression for G in terms of sine and cosine integrals can also be found in Refs. 2a and 3.

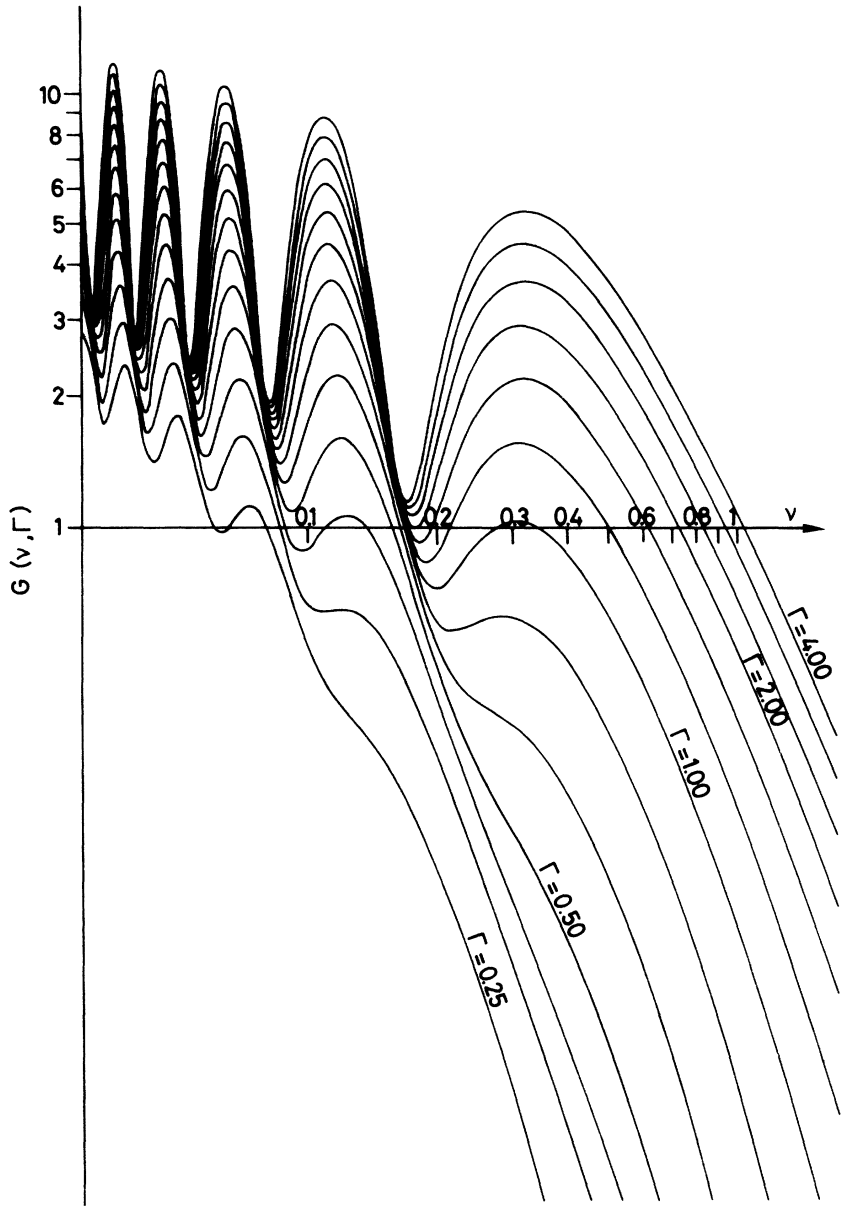

FIG. 5. The universal function $G(\nu, \Gamma)$ which gives the single-foil yield. Logarithmic scales. The Γ's are in a geometrical progression of ratio $2^{1/3}$.

3. *Case where there is incoherent addition from the two surfaces*

The interference between the two single-surface amplitudes is washed out by integration in θ if

$$a \gg l_1, \quad \text{i.e.,} \quad l_1 \gg Z_2 . \tag{3.35}$$

In the vacuum case, this reduces to $\nu \gg \Gamma^2$ (see Fig. 4).

We can also neglect the interference effect if we further integrate over the photon frequency in the region $\nu \ll 1$. In this case the domain of $V = \nu^{-1}$ extends very far and the interference factor in (3.23) can again be replaced by its mean value. Then we can substitute for (3.35) the weaker condition

$$l_1 \gg Z_1 . \tag{3.36}$$

4. *Case of constructive interference; optimization of the total yield*

In Eq. (3.25) the single-surface term has a maximum at $y = y_{\max}$ with

$$4a/3 < y_{\max} < 2a . \tag{3.37}$$

We have enhancement if $\varphi_{1\max} \equiv y_{\max} + V$ is not far from π, 3π, etc., and reduction if $\varphi_{1\max} \simeq 0, 2\pi$, etc. For $a \ll 1$, i.e., $\Gamma \gg \sqrt{\nu}$, we have $\varphi_{1\max} \simeq \nu^{-1}$; therefore, the function $G(\nu, \Gamma)$ has ridges at $\nu^{-1} = \pi, 3\pi$, etc., and valleys at $\nu^{-1} = 2\pi, 4\pi$, etc. (see Fig. 5). We can take advantage of the ridge at the "magic value"

$$\nu = 1/\pi \tag{3.38}$$

for the optimization of the total yield. The foil thickness and the central frequency $\bar{\omega}$ of the x-ray detector must be such that

$$\bar{\omega} \simeq \omega_1/\pi = l_1 \omega_{P1}^2/2\pi . \tag{3.39}$$

The other ridges are much less interesting because their band width in ω is smaller and there is more absorption. The height of a ridge increases logarithmically with Γ:

$$G(\text{ridge}) \simeq \ln(\Gamma^4/\nu^3) - 3 - C \tag{3.40}$$

($C = 0.577\ldots$), while the valleys stay at

$$G(\text{valley}) \simeq C - 1 - \ln\nu . \tag{3.41}$$

To be complete, in the formation-zone "plain," we have

$$G \sim \nu^{-2}[\ln(\Gamma^2/\nu) - C + \tfrac{1}{2}]/2 . \tag{3.42}$$

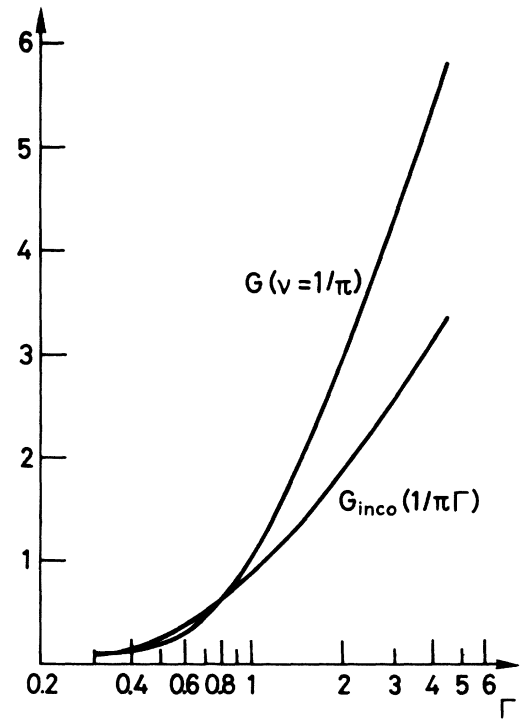

FIG. 6. Compared semilog plots of G_{inco} and $G(\nu = 1/\pi, \Gamma)$.

For $a \sim 1$, i.e., $\Gamma \sim \sqrt{\nu}$, $\varphi_{1\max}$ depends also on Γ, and the ridges and valleys are curves in the (ν, Γ) plane. This can increase the γ dependence of the yield (see the curve for $\nu = 1/\pi$, Fig. 6, where we pass from destructive interference for $0.35 < \Gamma < 0.75$ to constructive interference for $\Gamma > 0.8$).

5. *Saturation of the total energy radiated in the nonvacuum case*

The presence of a frequency cutoff at $\omega \simeq \omega_1$, as we have seen in Sec. III B 1, changes the linear dependence of $W(\gamma)$ into a logarithmic one when $\Gamma \sim 1$. This is true as long as we can neglect ξ_2 in (3.1), i.e., for $\omega > \gamma\omega_{P2}$ or $\nu > \Gamma\gamma^{1/2}$, otherwise we have saturation. As ν is practically limited by 1, we have a complete saturation of W when $\Gamma\gamma^{1/2} \gtrsim 1$. In fact, the main contribution to W comes from the region $\nu \sim 1/\pi$; therefore the saturation is rather given by

$$\Gamma = \bar{\Gamma}_{\text{sat},d} \sim \gamma^{-1/2}/\pi ,$$

i.e., (3.43)

$$\gamma = \bar{\gamma}_{\text{sat},d} \sim \omega_1/\pi\omega_{P2} .$$

(The subscript d recalls that this saturation comes from the nonzero gas density.)

C. The "single-gap" yield. Saturation phenomena

Before studying the N-foil case, it is instructive to study the yield produced by an isolated gap; the N-foil yield shares some properties of the single-foil yield and some of the single-gap yield. Moreover, the yield from a foam also has these properties.

The interference factor is now

$$4\sin^2(\varphi_2/2) = 4\sin^2[(\gamma^{-2} + \theta^2 + \xi_2^2)\omega l_2/4] . \tag{3.44}$$

Taking $z = \varphi_2$ as the integration variable, the yield can be written, similarly to (3.25),

$$\left(\frac{dW}{d\omega}\right)_{\text{single gap}} = \frac{2\alpha}{\pi}\int_b^\infty (z-b)\,dz\left(\frac{1}{z} - \frac{1}{z+V_2}\right)^2 2\sin^2(z/2)$$

$$= \frac{2\alpha}{\pi} G_{\text{gap}}(b, V_2) , \tag{3.45}$$

where

$$b = (\gamma^{-2} + \xi_2^2)\omega l_2/2 = l_2/Z_2 \tag{3.46}$$

and

$$V_2 = (\xi_1^2 - \xi_2^2)\omega l_2/2 = l_2/Z_1 - l_2/Z_2 . \tag{3.47}$$

The single-surface term in (3.45) has a peak at z between $4b/3$ and $2b$ [cf. (3.37)], of width $\sim b$. It

has also a tail extending up to

$$b + V_2 = (\gamma^{-2} + \xi_1^2)\omega l_2/2 = l_2/Z_1 . \quad (3.48)$$

From (3.45) we deduce the following features.

(i) We have $G_{\text{gap}} < 2G_{\text{inco}}$; therefore, if $\omega \gg \gamma\omega_{P1}$, i.e., $\eta \gg 1$, the yield is very low.

(ii) The yield is also negligible if

$$l_2 \ll Z_1 . \quad (3.49)$$

This is a formation-zone effect in the gap [$l_2 \ll z_2(\theta)$ in the relevant θ range]. Note the lack of symmetry between this condition and the condition $l_1 \ll Z_1$ for the single-foil formation-zone suppression.

(iii) If $\gamma \gg \omega/\omega_{P2}$, then b does not depend any more on γ and we have the saturation predicted by (3.5)

$$\gamma_{\text{sat},d} \simeq \omega/\omega_{P2} . \quad (3.50)$$

(iv) In the vacuum case, b goes to zero when $\gamma \to \infty$ but G_{gap} remains finite. This saturation is due to the formation-zone effect in the gap ($l_2 \ll Z_2$). Let us define a "saturation energy" $\gamma_{\text{sat},FZ}$ by

$$G_{\text{gap}}(\gamma = \infty) = G_{\text{inco}}(\gamma = \gamma_{\text{sat},FZ}) . \quad (3.51)$$

For large V_2 (which is the usual case), we find

$$\gamma_{\text{sat},FZ} \simeq e^{C+1/2}(l_2\omega/2)^{1/2} \simeq 2.2(l_2\omega/2)^{1/2}$$
$$\simeq 110(\omega/\text{keV})^{1/2}(l_2/\text{micron})^{1/2} . \quad (3.52)$$

In the nonvacuum case, although Z_2 is smaller, the saturation energy is not higher, because the other source of saturation takes place; in fact, G_{gap} is a decreasing function of ω_{P2}. Let us write

$$\gamma_{\text{sat}} = \min(\gamma_{\text{sat},d}, \gamma_{\text{sat},FZ}) . \quad (3.53)$$

(v) If b is large, the interference factor can be averaged out; therefore

$$l_2 \gg Z_2 \Rightarrow G_{\text{gap}} \simeq G_{\text{inco}} . \quad (3.54)$$

(vi) Contrary to the single-foil case, there is no oscillation in the ω spectrum; G_{gap} is most likely a monotonic decreasing function of ω: For $\omega > \gamma\omega_{P2}$, this can be proved by differentiating (3.45); for $\omega < \gamma\omega_{P2}$, we can replace γ by γ_{sat} which brings us in a region where G is not very different from G_{inco}.

The different regions where the above phenomena occur are shown in Fig. 7.

D. The stack of foils

The new feature which comes in when we add many identical foils at regular spacing is the presence of sharp peaks in the angular distribution of x rays because of N-foil interference. The peaks are at angles which satisfy the "resonance condition"

$$\varphi_1 + \varphi_2 \simeq \omega(l_1 + l_2)/v - (k_1 l_1 + k_2 l_2)\cos\theta = 2p\pi \quad (3.55)$$

(p integer). The spacing between the peaks is given by

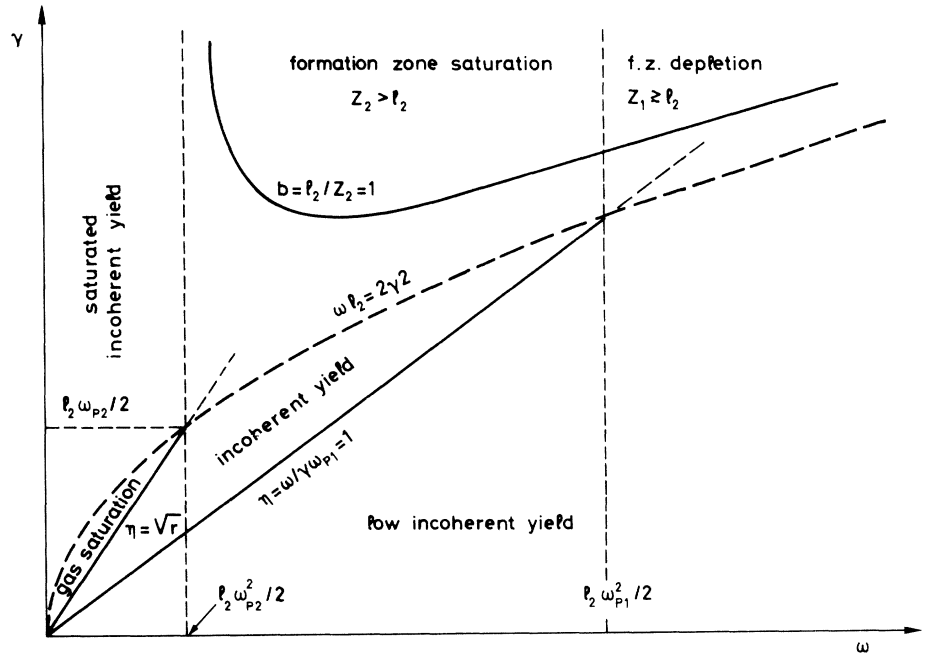

FIG. 7. Different regions of the ω, γ plane relevant for the single-gap yield.

$$\Delta\cos\theta \simeq \lambda/(l_1+l_2), \tag{3.56}$$

which is a small quantity. Therefore it is difficult to separate them experimentally. Even if we did it, their positions could not provide a precise measurement of γ. So we are again interested in the flux integrated over angles.

1. Symmetric role played by the gap and the foil

Let us consider the N-foil interference factor given by (2.16) or (2.19). Its average value, which we call "effective number of foils" is

$$N_{\text{eff}} = (1-e^{-N\sigma})/(1-e^{-\sigma}). \tag{3.57}$$

From now on, we shall consider only situations where N_{eff} is large, i.e., many foils and little absorption in one foil. In this case, $I^{(N)}$ can be approximated by a sum of δ functions:

$$I^{(N)}(\varphi_{12},\sigma) \simeq 2\pi N_{\text{eff}} \sum_p \delta(\varphi_{12}-2p\pi). \tag{3.58}$$

We can therefore replace the single-foil interference factor $4\sin^2(\varphi_1/2)$ by $4\sin^2(\varphi_2/2)$, thus having a formal symmetry between foils and gaps.

2. Saturation

In particular, the N-foil yield suffers the same saturation as does the single-gap yield, and the same ω cutoff as does the single-foil yield. Let us introduce the new dimensionless parameter

$$\tau = l_2/l_1. \tag{3.59}$$

Equations (3.53), (3.50), and (3.52) can be rewritten

$$\Gamma_{\text{sat}} = \min(\Gamma_{\text{sat},d}, \Gamma_{\text{sat},FZ}), \tag{3.60}$$

$$\Gamma_{\text{sat},d} = \nu\gamma^{-1/2}, \tag{3.61}$$

$$\Gamma_{\text{sat},FZ} \simeq 2.2(\tau\nu)^{1/2}. \tag{3.62}$$

As the major part of the energy radiated W comes from the region $\nu \sim 1/\pi$, we have typically[9]

$$\bar{\Gamma}_{\text{sat}} \simeq \gamma^{-1/2}/\pi, \text{ i.e., } \bar{\gamma}_{\text{sat}} = \omega/\pi\omega_{P2}$$

if

$$\tau\gamma \simeq \rho_2 l_2/\rho_1 l_1 > 1/15 \tag{3.63}$$

and if $\tau\gamma < 1/15$

$$\bar{\Gamma}_{\text{sat}} \simeq 1.2\tau^{1/2}, \text{ i.e., } \bar{\gamma}_{\text{sat}} \simeq 0.6\omega_{P1}(l_1 l_2)^{1/2}. \tag{3.64}$$

The numerical coefficients appearing in these formulas must not be taken too seriously; other definitions of γ_{sat} may differ by factors of order 3. Furthermore, the coefficient 2.2 in (2.62) is only an average on ν.

Experimentally, the formation-zone effect in the gap has been confirmed by reducing the foil spacing to some tenth of a millimeter.[8] Saturation phenomena have been observed also by other groups,[10,4] but they are also partly due to the gap being air.

3. Analysis of the interference effect with the use of the (φ_1, φ_2) plane

By means of (3.58), we can factorize the dependence on the absorption parameters and on N:

$$\left(\frac{dW}{d\omega}\right)_{N \text{ foil}} = \frac{2\alpha}{\pi} N_{\text{eff}} G_{\text{many}}. \tag{3.65}$$

The N-foil interference factor in G_{many} depends only on $\varphi_{12} = \varphi_1 + \varphi_2$ with $\varphi_1 = y + V$ and, from (2.10), (3.29), and (3.59)

$$\varphi_2 = \tau y. \tag{3.66}$$

Instead of (3.25) we have now

$$G_{\text{many}} = \int_a^\infty (y-a)\,dy \left(\frac{1}{y} - \frac{1}{y+V}\right)^2 2\sin^2\frac{y+V}{2}\,2\pi \times \sum_p \delta(\varphi_{12}-2p\pi). \tag{3.67}$$

In the case of vacuum gaps, we can write

$$G_{\text{many}} = G_{\text{many}}(\nu, \Gamma, \tau) \tag{3.68}$$

and in the general case

$$G_{\text{many}} = G_{\text{many}}(\nu', \Gamma', \tau), \tag{3.68'}$$

where ν' and Γ' have been defined by (3.33) and (3.34). Thus the photon spectrum is essentially a function of only three variables.

Equation (2.10) defines a semistraight line Ax of slope τ in the (φ_1, φ_2) plane (Fig. 8). The position of the running point $M = (\varphi_1, \varphi_2)$ on this line can be taken as the integration variable, instead of y, and we get

$$G_{\text{many}} = \int_0^\infty s_{AM}\,ds_{AM} \left(\frac{1}{s_{MP}} - \frac{1}{s_{MQ}}\right)^2 (1-\cos\varphi_1)2\pi \times \sum_p \delta(\varphi_1+\varphi_2-2p\pi), \tag{3.69}$$

when s_{CD} denotes the distance between points C and D. The coordinates (φ_1, φ_2) of P, Q, A, and M are

$$P \begin{cases} V = (1-\gamma)\nu^{-1} \\ 0, \end{cases} \tag{3.70}$$

$$Q \begin{cases} 0 \\ -\tau V, \end{cases} \tag{3.71}$$

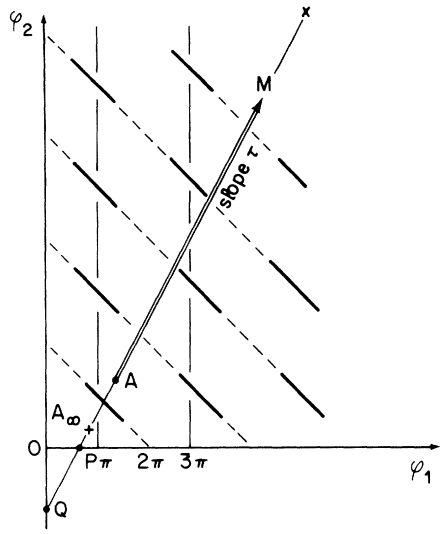

FIG. 8. The path of integration of formula (3.69) in the φ_1, φ_2 plane. Dark segments indicate constructive single-foil interference.

$$A\begin{cases} V + a = \nu^{-1} + \nu\Gamma^{-2} = l_1/Z_1 \\ \tau a = \gamma\tau\nu^{-1} + \tau\nu\Gamma^{-2} = l_2/Z_2\,, \end{cases} \tag{3.72}$$

$$M\begin{cases} V + y \\ \tau y\,. \end{cases} \tag{3.73}$$

Because of the δ functions, the integration in (3.69) is a summation of the single-foil amplitude over the intersection points between Ax and the lines $\varphi_1 + \varphi_2 = 2p\pi$. The quantity

$$s_{AM}\left(\frac{1}{s_{MP}} - \frac{1}{s_{MQ}}\right)^2 \tag{3.74}$$

represents the single-surface intensity. It is peaked at about $s_{AM,\max} \sim s_{PA}$ and has a significant tail up to $s_{AM,\text{tail}} \sim s_{QA}$. The single-foil interference factor $1 - \cos\varphi_1$ is greater than 1 on the dark segments and smaller than 1 on the thin segments. It is not periodic in p but its average value is 1. The whole PQ straight line does not depend on γ. The starting point A goes downward towards A_∞ when Γ increases.

The most important qualitative features of the N-foil yield can be deduced simply by looking at the position of Ax. We state here the main results.

(i) When $\Gamma \to \infty$,

$$A \to A_\infty = \begin{cases} \nu^{-1} \\ \gamma\tau\nu^{-1}\,, \end{cases} \tag{3.75}$$

then $G \to$ constant. We find again the two types of saturation discussed in III D 2: formation-zone effect if A_ω lies below the line $\varphi_2 = 1$, gas-density effect in the opposite case.

(ii) To increase γ, i.e., the gas density, make a translation of Ax upward. Most likely, this reduces the yield [cf. (3.4)].

(iii) Condition for neglecting the N-foil interference effects: Suppose that τ is large and $s_{PA} \gtrsim 2\pi$, which implies $\tau a = l_2/Z_2 \gtrsim 2\pi$. Then neither the single-foil interference factor nor the single-surface amplitude changes appreciably between two points. We conclude

$$l_2 \gtrsim 2\pi Z_2 \Rightarrow G_{\text{many}} \simeq G(\nu, \Gamma)\,, \tag{3.76}$$

at least for big τ. This last condition will be relaxed below.

(iv) Conditions for neglecting any interference effect: Suppose that both projections of s_{PA} are large:

$$a = l_1/Z_1 \gtrsim 2\pi \tag{3.77}$$

and

$$\tau a = l_2/Z_2 \gtrsim 2\pi\,; \tag{3.78}$$

then the average value of $1 - \cos\varphi_1$ over a length equal to $s_{PA}/2$ is not far from 1. As, over the same length, the single-surface amplitude does not vary too much, we can say

$$G_{\text{many}} \simeq G_{\text{inco}}(\eta) \simeq G\,. \tag{3.79}$$

The case $l_2 > 2\pi Z_2$, $\tau \lesssim 1$ is a special case of (3.77) and (3.78). This relaxes the condition of τ large in (iii).

(v) Threshold effects. As γ increases, A goes through successive lines $\varphi_1 + \varphi_2 = 2p\pi$. Each time it occurs, a new ring appears in the angular distribution of the x rays, and this produces a break in the slope of $dW/d\omega$ versus γ. These "thresholds" are given by

$$\varphi_{12}(A) \equiv \nu(1+\tau)\Gamma_{\text{thr}}^{-2} + (1+\gamma\tau)\nu^{-1} = 2p\pi\,. \tag{3.80}$$

The relative size of this effect will be important if s_{PA} and s_{QA} are small, and we can have a threshold detector based on this effect. The best is to choose the line $\varphi_{12} = 2\pi$ and to cross it at $\varphi_1 \simeq \pi$, with A_∞ close to P (low gas density). P must not be too close to the origin (the yield vanishes if P and Q are in 0), i.e., $\nu \lesssim 2/\pi$, and τ must not be too big (for very large τ, the other δ functions make an important background). Figure 9 shows some examples of these thresholds.

(vi) For practical purposes, we have to integrate the detected yield in ν over the band width of the x-ray detector. As Γ_{thr} depends on ν, this will wash out somewhat the threshold, unless Γ_{thr} is stationary in ν. This is equivalent to saying that $\varphi_{12}(A)$ [Eq. (3.80)] is stationary in ν. Then the "space term" is equal to the "mass term":

$$\nu(1+\tau)\Gamma^{-2} = (1+\gamma\tau)\nu^{-1} = p\pi\,, \tag{3.81}$$

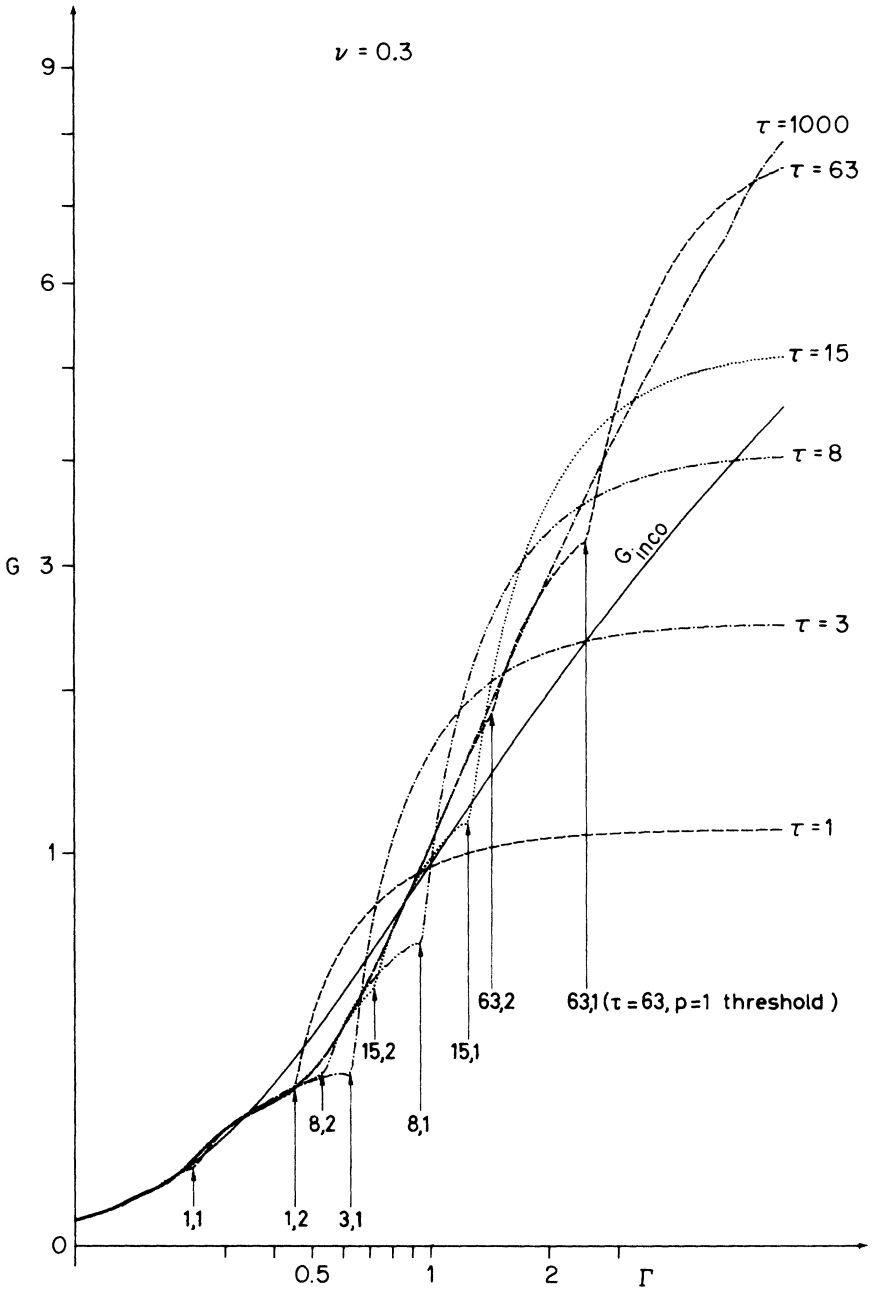

FIG. 9. The function $G_{many}(\nu = 0.3, \Gamma, \tau)$ for different values of τ. We use a logarithmic scale for Γ and a square-root scale for G. Only the $p = 1$ and $p = 2$ thresholds [Eq. (3.80)] are apparent on these curves.

$$\nu = (1 + r\tau)/p\pi = \nu_{sta}, \tag{3.82}$$

$$\Gamma = (1 + \tau)^{1/2}(1 + r\tau)^{1/2}/p\pi = \Gamma_{sth}. \tag{3.83}$$

Figure 10 shows the stationarity of Γ_{thr}.

Let us assume $r\tau$ ($\simeq$ gap mass/foil mass) $\ll 1$, then the $p = 1$ stationary threshold is given by

$$\nu_{sta} = 1/\pi, \tag{3.84}$$

$$\Gamma_{sth} = (1 + \tau)^{1/2}/\pi. \tag{3.85}$$

ν_{sta} happens to have the "magic value" introduced in III B 4. We see that this stationary threshold is not an exceptional case. In fact, most experiments are made around $\nu \sim 1/\pi$, and if τ is not too big, the threshold is within the experimental range of Γ. This is the case, for instance, in Ref. 4.

We point out that the condition to have a large threshold effect, established in V, and the condition for stationarity are compatible and, in fact,

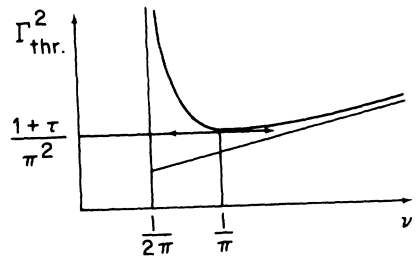

FIG. 10. $p=1$ threshold position, as a function of ν, in the vicinity of $\nu=1/\pi$ (in the vacuum case).

are simultaneously satisfied if τ is neither too low (let us say $\tau \gtrsim 3$) nor too large. But we must also verify that the ratio

$$\Gamma/\nu = \gamma\omega_{P1}/\omega = 1/\eta\,, \tag{3.86}$$

which governs the single-surface yield, is not too low at $\Gamma=\Gamma_{thr}$; let us say $\Gamma \gtrsim 1$ whence $\tau \gtrsim 8$.

For larger τ, the height of the step stays about the same but the background is higher (see Fig. 9). Figure 11(b) shows the stationary threshold effect expected from a radiator of 1000 Berylium foils, 1 mil (25 μm) in thickness, including absorption. The x-ray detector is supposed to have an efficiency equal to 1 in the range 10 to 24 keV and zero elsewhere ($\omega_1/\pi \simeq 14$ keV). We see that

$$3 \lesssim \tau \lesssim 8 \tag{3.87}$$

are good values for observing the stationary threshold effect.

From a theoretical point of view, the threshold would be the clearest manifestation of the N-foil interference effect[11] (formation-zone effect in the gap is only a manifestation of the "single-gap" interference effect and could be observed in nonperiodic medium, such as sytrofoam, as well). The position of the threshold is not affected by absorption or by the imperfect x-ray detection. The agreement between the experimental value of the threshold and formula (3.83) or (3.85) would constitute a relatively precise test of the formula

$$\epsilon(\omega) = 1 - 4\pi\alpha n_e/m_e\omega^2\,, \tag{3.88}$$

which results from (2.1) and (2.2). Returning to the usual quantities ω and γ, (3.82) and (3.83) become

$$\omega_{sta} = (l_1\omega_{P1}{}^2 + l_2\omega_{P2}{}^2)/2\pi$$
$$\simeq 3\times 10^3(\rho_1 l_1 + \rho_2 l_2)\ \text{keV/g cm}^{-2}\,, \tag{3.82'}$$

$$\gamma_{sth} = (l_1+l_2)^{1/2}(l_1\omega_{P1}{}^2 + l_2\omega_{P2}{}^2)^{1/2}/2\pi\,. \tag{3.83'}$$

This test does not need a precise determination of the x-ray frequency, because the threshold is stationary with respect to ω.

For the applications, we have the possibility to build a *threshold detector*, analogous to Čerenkov threshold detectors, but working at higher γ. It could discriminate pions from kaons *or* (perhaps) kaons from protons in a beam of given energy. One single detector could not discriminate simultaneously pions, kaons, and protons: We have only one important threshold per radiator, and soon above this threshold, we have saturation; comparison of (3.46) and (3.85), or Fig. 11 indicates

$$\gamma_{sat,FZ} \sim (3\pm 1)\gamma_{sth}\,. \tag{3.89}$$

The gas-density effect strongly reduces the threshold effect if

$$r\tau \simeq \text{gap mass/foil mass} \gtrsim 1\,. \tag{3.90}$$

Indeed, with $r\tau=1$, there is no more $p=1$ threshold for $\nu=1/\pi$ [Eq. (3.80)]. There is still a stationary threshold at $\nu=2/\pi$, $\Gamma \sim (2\tau)^{1/2}/\pi$ but it is not far from the saturation region.

(vii) As in the single-foil case, we expect oscillations in ν governed by the φ_1 of M_{max}. These are apparent in Fig. 12. The oscillations are very rapid when $\nu^{-1} \gg 1$ (which implies $l_1 \gg Z_1$).

Integrating over a wide enough frequency range where

$$l_1 \gtrsim 2\pi Z_1 \tag{3.91}$$

gives us the *single-gap* yield (instead of the single-surface yield as in Sec. III B 3).

(viii) There are also breaks in the x-ray spectrum at fixed γ; when, while scanning in ω, ν reaches a root of Eq. (3.80), a new ring appears in the angular distribution, thus producing a break. Then, the opening angle 2θ of the ring grows, reaches a maximum when $\nu=\nu_{sta}$ [Eq. (3.82)], and goes back to zero at the other root of Eq. (3.80), giving another break. The angle θ is given by

$$\gamma^{-2} + \theta^2 = \gamma_{thr}{}^{-2}\,. \tag{3.92}$$

If one wants to observe the ring, it is best to choose $\nu \sim \nu_{sta}$ (because of the stationarity).

These breaks in the ω spectrum cannot be very spectacular: Let us take $p=1$, to have a good yield, and $r=0$. If Γ is just above Γ_{sth}, the two breaks are very close together and the contribution of the $p=1$ ring has no time to get large between them. On the other hand, if $\Gamma \gg \Gamma_{sth}$, the breaks are at $\nu=1/2\pi$ and $\nu=\infty$, and the $p=1$ contribution vanishes at these points. Figure 12 shows that, indeed, the N-foil spectrum does not look very different from the single-foil spectrum (except for saturation). Furthermore, the breaks can be washed out by the finite width of the x-ray

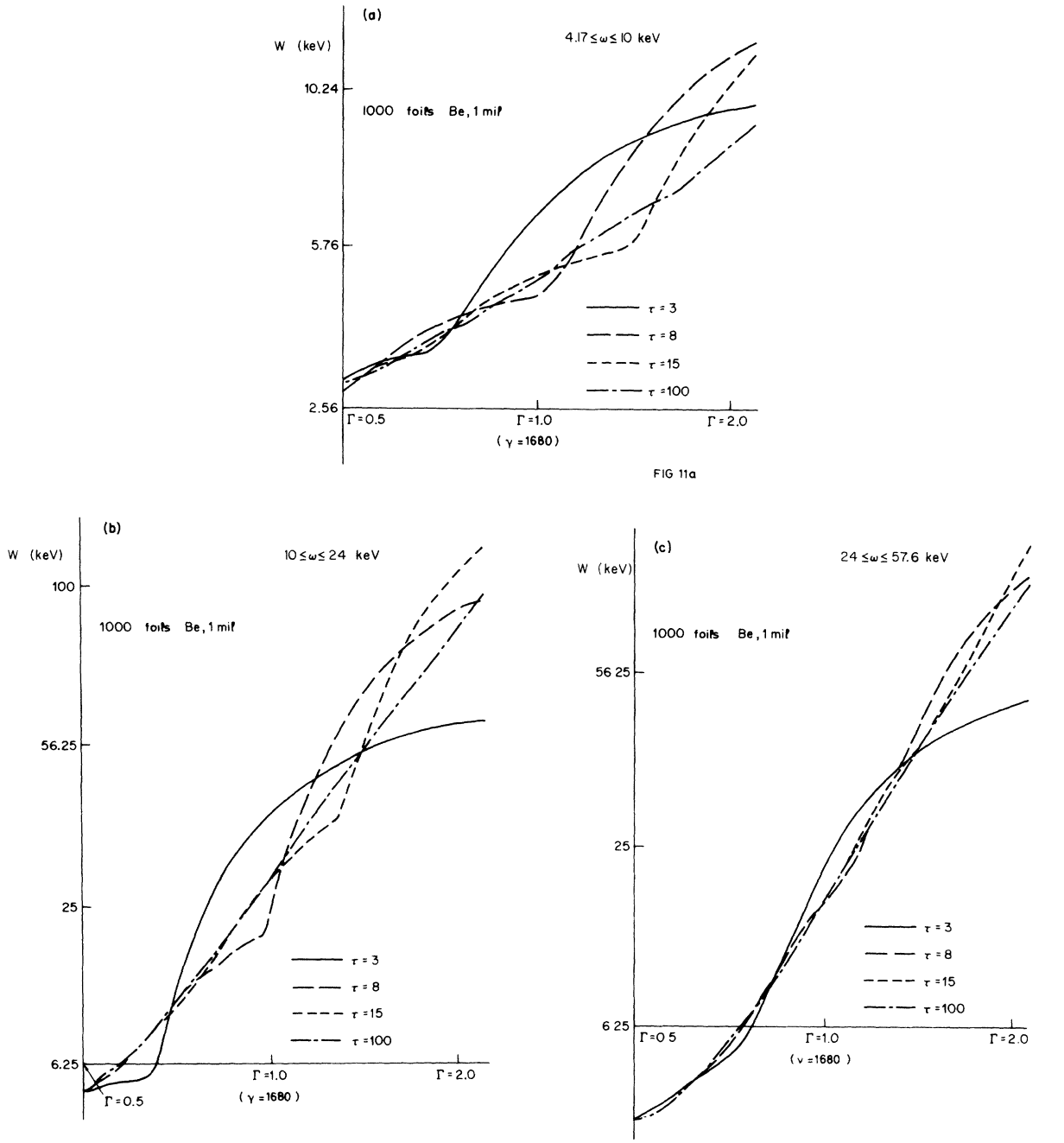

FIG 11a

FIG. 11. Yield integrated with the absorption factor N_{eff} in three different band widths, from 1000 beryllium foils 1 mil thick and four values of τ. The intermediate band width contains the stationary frequency $\omega_1/\pi \simeq 14.4$ keV. $\Gamma = \gamma/\gamma_1$ with $\gamma_1 = 1680$. A logarithmic scale is used for Γ and a square-root scale for W.

detector. These facts could explain why they have not been observed yet.

(ix) Magnitude of the n-foil enhancement. Although the N-foil interference effect can greatly modify the slope of $dW/d\omega$ versus γ, it cannot enhance G_{many} by more than a factor two relative to G_{inco}: Enhancement occurs when a δ function coincides with the peak of the single-surface term in (3.69). If A is far from the φ_1 axis, this peak is too broad and we get the single-foil yield; if A is close to the φ_1 axis, the peak can be narrow, but the $\sin^2(\varphi_2/2)$ factor kills it.

To conclude, the N-foil yield shares properties of the single-surface yield (cutoff frequency $\gamma\omega_{P1}$, gas saturation at $\gamma = \omega/\omega_{P2}$), of the single-foil yield (formation-zone depletion when $\nu > 1$, oscil-

lations, biggest contribution of $\nu \sim 1/\pi$), and of the single-gap yield (formation-zone saturation). In addition, it has singularities in the form of thresholds, which constitute a typical N-foil interference effect, and affects strongly the γ dependence for $\nu \sim 1/\pi$.

Let us recall also the condition for neglecting some of the interference effects:

$$\left.\begin{array}{l} l_2 > 2\pi Z_2 \\ l_1 > 2\pi Z_1 + \text{integration in } \omega \\ l_1 > 2\pi Z_1, \quad l_2 > 2\pi Z_2 + \text{integration in } \omega, \text{ or} \\ l_1 \text{ and } l_2 > 2\pi Z_2 \end{array}\right\} \Rightarrow \sim \text{single surface},$$

$$l_2 > 2\pi Z_2 \Rightarrow \sim \text{single foil},$$

$$l_1 > 2\pi Z_1 + \text{integration in } \omega \Rightarrow \sim \text{single gap},$$

and the two meaningful values of Γ

$$\bar{\Gamma}_{\text{sat}} = \min(1.2\tau^{1/2}, \gamma^{-1/2}/\pi),$$

$$\Gamma_{\text{sth}} = (1+\tau)^{1/2}/\pi \quad (\text{for } \gamma = 0).$$

IV. CONCLUSIONS AND MISCELLANEOUS PROBLEMS

This study has shown that for a practical radiator, N-foil interference effects cannot be neglected, and even can be used to improve the sensitivity to γ. Formation-zone effect in the foils fix a lower limit to their weight [Eq. (3.22)] and formation-zone saturation in the gap imposes a minimum spacing, according to (3.52) or (3.64). The gas density has always a negative effect and must not exceed a certain value, fixed by (3.43). The single-foil interference is mainly seen in the ω spectrum (oscillations), while the N-foil interference is mainly seen in the γ dependence, in the form of thresholds.

Some important problems have not been treated. Let us discuss them briefly.

Irregularities in the foil spacing or thickness

If l_1 or l_2 is not constant but continuously varying between the front and the bottom of the radiator, the threshold [Eq. (3.83′)] can be smeared out. out. But if they have only short-range fluctuations, the destruction of coherence is not too important.

Let us define N_{coh} ($\leq N_{\text{eff}}$) as the maximum number of consecutive foils that can interfere coherently in the forward direction and ψ_{ij} the phase shift between the ith and the jth at $\theta = 0$

$$\psi_{ij} = \sum_{m=i}^{j-1} \varphi_m . \tag{4.1}$$

Coherence is lost when the fluctuations

$$\Delta\psi_{ij} \gtrsim \pi/2 . \tag{4.2}$$

In the case where the foil thickness has fluctuations $\sim l_1\Delta$, we have (assuming $\gamma\tau \ll 1$ and stationarity, $\nu \simeq 1/\pi$)

$$\Delta\psi_{ij} = (j-i)^{1/2}\Delta\varphi_1 , \tag{4.3}$$

$$\Delta\varphi_1 = \Delta l_1 \omega_{P_1}{}^2/2\omega = \pi\Delta l_1/l_1 , \tag{4.4}$$

whence

$$N_{\text{coh}} = (l_1/\Delta l_1)^2/4 . \tag{4.5}$$

In the case where the spacing has fluctuations $\sim \Delta l_2$, we get a similar result if these fluctuations are uncorrelated. But this is not the usual case: More likely, the random errors are in the positions of the foils with respect to their ideal positions. Then $\Delta\psi_{ij} = \omega\gamma^{-2}\Delta(l_i + \cdots + l_{j-1})$ does not grow with $j - i$ and N_{coh} is N_{eff}.

To calculate the yield, we can group the foils in packets of N_{coh} (perhaps $2N_{\text{coh}}$?) foils and neglect the interference effects between different packets. The peaks of the N-foil interference factor $I^{(N_{\text{coh}})}(\varphi_{12})$ have then a finite width

$$\delta\varphi_{12} = 2\pi/N_{\text{coh}} . \tag{4.6}$$

This induces a finite width for the rings of the angular distribution and a spread of γ_{thr} given by [see (3.80)]

$$\nu(1+\tau)\Delta(\Gamma_{\text{thr}}{}^{-2}) = \delta\varphi_{12} ; \tag{4.7}$$

using (3.81), we get

$$\Delta\Gamma_{\text{sth}}/\Gamma_{\text{sth}} = \Delta\gamma_{\text{sth}}/\gamma_{\text{sth}} = 1/N_{\text{coh}} \tag{4.8}$$

(perhaps $1/2N_{\text{coh}}$?). Finally,

$$\Delta\gamma_{\text{sth}}/\gamma_{\text{sth}} \sim 4(\Delta l_1/l_1)^2 . \tag{4.9}$$

We see that the loss of coherence is a second-order effect in Δl_1. A radiator with $\Delta l_1/l_1 \sim 3/100$ has $\Delta\gamma_{\text{sth}}/\gamma_{\text{sth}} \sim 1/100$ only.

Multiple scattering

The fact that the charged particle does not follow a straight-line trajectory, because of Coulomb scattering by the nuclei, may destroy the N-foil interference for two reasons:

(i) the peaks of the angular distributions from the mth foil and the nth foil do not overlap for large $|m-n|$; and

(ii) the phase difference between these two foils is increased by random quantity because be-

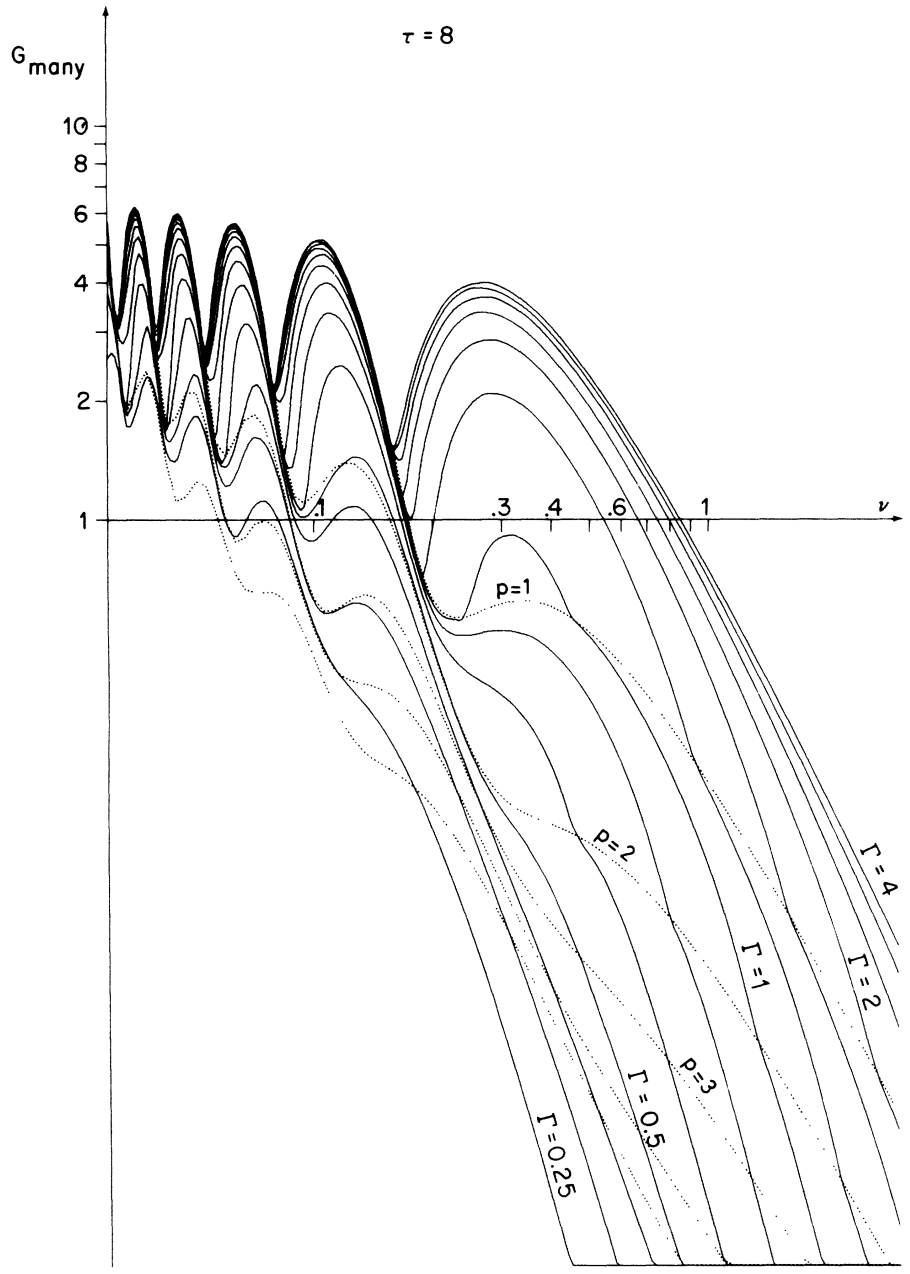

FIG. 12. The function $G_{\text{many}}(\nu, \Gamma, \tau = 8)$ for different values of Γ. Same scales as in Fig. 5. In dotted lines are plotted the quantities $G_{\text{many}}(\nu, \Gamma_{\text{thr}}, \tau)$, where Γ_{thr} are given by (3.80). They represent the breaks of the G, ν, Γ surface.

tween them, the particle is retarded with respect to a rectilinear motion.

As in the preceeding problem, we have to evaluate N_{coh}. Let us call β_{ms} the deflection of the particle resulting from multiple scattering and β_{ss} a single scattering angle:

$$\beta_{ms} = \sum \beta_{ss} . \tag{4.10}$$

The overlap condition (i) is

$$\beta_{ms} \lesssim \gamma^{-1} \tag{4.11}$$

and the phase condition (ii) is

$$\omega \delta l \lesssim \pi/2 . \tag{4.12}$$

δl is the elongation of the particle trajectory between the two foils considered. To estimate it, one can assume that only one single scattering

angle is important in the sum (4.10). Then

$$\delta l \sim l\beta_{ms}^2/8\,; \tag{4.13}$$

condition (4.12) becomes

$$|m-n|\,\omega(l_1+l_2)\beta_{ms}^2 \lesssim 4\pi\,. \tag{4.14}$$

But we are interested in the stationary threshold case, where [cf. (3.81)]

$$\omega(l_1+l_2)\gamma_{\rm sth}^{-2} = 2\pi\,; \tag{4.15}$$

whence the second limitation

$$|m-n|\,\beta_{ms}^2 \lesssim 2\gamma^{-2}\,, \tag{4.16}$$

which is stronger than (4.11).

The problem is to estimate β_{ms}. For single scattering, the differential cross section is well represented by[12]

$$d^2\sigma \begin{cases} = (2Z\alpha/E)^2 d^2\tilde{\beta}(\beta^2+\beta_{\rm min}^2)^{-2}, & \beta<\beta_{\rm max} \\ = 0, & \beta>\beta_{\rm max}. \end{cases} \tag{4.17}$$

$\beta_{\rm min}$ is the cutoff due to the screening by the atomic electrons, and $\beta_{\rm max}$ is the one due to the finite nuclear size:

$$\beta_{\rm min} r_a = \beta_{\rm max} r_N = 1/E\,, \tag{4.18}$$

with

$$r_a^{-1} \simeq m_e \alpha Z^{1/3}\,, \tag{4.19}$$

$$r_N \simeq 1.2\ \text{Fermi} \times A^{1/3}\,. \tag{4.20}$$

For the multiple scattering angle after z collisions, we have at our disposal the following formulas:

$$\langle\beta_{ms}^2\rangle = z\beta_{\rm min}^2 \ln(\beta_{\rm max}^2/e\beta_{\rm min}^2)\,, \tag{4.21}$$

$$\langle\beta_{ms}\rangle \simeq z^{1/2}\beta_{\rm min}\{1.45+0.8[\ln(z/6)]^{1/2}\}\,, \tag{4.22}$$

and a semiempirical formula[13]

$$\tilde{\beta}_{ms}^2 \simeq z\beta_{\rm min}^2(1+0.75\ln z)\,, \tag{4.23}$$

where $\tilde{\beta}_{ms}$ denotes the mode of the β_{ms} distribution:

$$\text{prob}(\beta_{ms} > \tilde{\beta}_{ms}) = \tfrac{1}{2}\,. \tag{4.24}$$

Formulas (4.22) and (4.23) are valid as long as

$$z\beta_{\rm min}^2/\beta_{\rm max}^2 \sim \text{mean number of hard collisions} \ll 1\,. \tag{4.25}$$

For our problem, the typical value of β_{ms} is given by (4.22) or (4.23) rather than (4.21). This is because a hard collision ($\beta \sim \beta_{\rm max}$) is very improbable (although it contributes to $\langle\beta^2\rangle$). In fact, the cross section for a hard collision is only

$$\sigma_{\rm hard} \sim \pi(2Zar_N)^2\,, \tag{4.26}$$

which is much less than a typical nuclear cross section. We shall take (4.23) (which gives $\tilde{\beta} \sim 0.8\langle\beta\rangle$ in a wide range of z).

From (4.17)–(4.19)

$$\sigma_{\rm tot} = \pi(2Z\alpha/E\beta_{\rm min})^2 = 4\pi m_e^{-2} Z^{4/3}\,. \tag{4.27}$$

This gives, for a quantity $L\rho$ of traversed matter

$$\begin{aligned} z\beta_{\rm min}^2 &= \pi L\rho\mathfrak{N}A^{-1}(2Z\alpha/E)^2 \\ &= Z\alpha E^{-2} m_e L\omega_P^2 \\ &= 0.6Z^2A^{-1}(\rho L/\text{g cm}^{-2})\, m_e^2/E^2 \end{aligned} \tag{4.28}$$

[the second expression comes from (2.2′)], and

$$\begin{aligned} z &= 4\pi Z^{4/3} m_e^{-2}\rho\mathfrak{N}L/A \\ &= Z^{1/3} L\omega_P^2(\alpha m_e)^{-1} \\ &= 2Z^{4/3}A^{-1}(\rho L/\text{g cm}^{-2}) \times 58000\,. \end{aligned} \tag{4.29}$$

Neglecting the gas contribution, we have

$$L\omega_P^2 = |m-n|\,l_1\omega_{P_1}^2 = 2|m-n|\,\omega_1 \tag{4.30}$$

and condition (4.16) can be written as

$$N_{\rm coh}^2 Z\alpha\omega_1 m_e m^{-2}[1+0.75\ln(2N_{\rm coh}\omega_1 Z^{1/3}/\alpha m_e)] = 1\,, \tag{4.31}$$

or, for electrons,

$$ZN_{\rm coh}^2\omega_1 \ln(2N_{\rm coh} Z^{1/3}\omega_1/\text{keV}) \simeq 10^5\ \text{keV}\,. \tag{4.31′}$$

For instance, with 25-micron-thick lithium foils ($\omega_1 = 11$ keV) $N_{\rm coh} = 21$, $\Delta\gamma_{\rm sth}/\gamma_{\rm sth} \sim 5\%$ (perhaps 2.5%?). For the sharpness of the threshold, lithium is the best material. For particles heavier than the electron, one can ignore multiple scattering.

Multiple scattering also modifies the single-surface yield[14-16] and is the source of bremsstrahlung. An interesting and open question is whether the total yield (modified transition radiation + bremsstrahlung) is affected by the N-foil interference, or only the transition radiation part.

Photon statistics

The differential yield $dW/d\omega\, d\Omega$ has been calculated classically. This is justified by the fact that the trajectory of the particle is not perturbed by the emission ($\omega \ll E$, unlike in hard bremmstrahlung), and the medium reacts coherently (is not heated) as in the Mossbaüer or Čerenkov effect. Thus we could consider the system particle plus radiator as a classical electromagnetic source. But the electromagnetic field must remain quantized because the number of photons is not very large ($\sim \alpha N_{\rm eff}$). W is only the average energy radiated when many particles of the same γ cross the radiator, and the number of emitted (also detected) photons follows a Poisson distribution:

$$\text{prob}(n_{\rm ph}) = \exp(-\langle n_{\rm ph}\rangle)\langle n_{\rm ph}\rangle^{n_{\rm ph}}/n_{\rm ph}!\,, \tag{4.32}$$

whose fluctuation is

$$\Delta n_{\rm ph} = \langle n_{\rm ph} \rangle^{1/2} . \tag{4.33}$$

If the photon frequency does not differ too much from $\bar{\omega}$, we have

$$W = \bar{\omega} \langle n_{\rm ph} \rangle , \tag{4.34}$$

$$\Delta W = \Delta n_{\rm ph} \bar{\omega} \simeq (W \bar{\omega})^{1/2} , \tag{4.35}$$

$$\Delta(W^{1/2}) \sim \bar{\omega}^{1/2}/2 . \tag{4.36}$$

Because of the fact that $\Delta(W^{1/2})$ and not ΔW is constant, it is convenient to take a square-root scale for W in the curve for W versus γ, in order to compare the γ resolution at different γ's. This has been done in Figs. 9 and 11.

Optimization of a detector

Many x-ray detectors are proportional counters, which have a linear response to the total energy deposited (except for fluorescent escape of x rays). The mean contribution of transition radiation is

$$W_{\rm det}(\gamma) = \frac{2\alpha}{\pi} \int d\omega\, G_{\rm many}(\nu, \Gamma, \tau) N_{\rm eff}(\omega) \epsilon(\omega) , \tag{4.37}$$

where $\epsilon(\omega)$ is the detector efficiency. If one is interested in the discrimination of two species of particles A and B of one given momentum, a threshold detector with $W_{\rm det}(\gamma_A)$ small and $W_{\rm det}(\gamma_B)$ large is convenient, and one might use the threshold effect. If one wants to measure γ over a range as large as possible, the threshold and saturation effects must be avoided by taking τ sufficiently large. In both cases, the optimization problem involves many parameters, but the choice has been greatly reduced by the above study. For instance, most of the radiated energy comes from the $\nu \sim 1/\pi$ peak; the output starts to be important at $\Gamma \sim 1$; saturation occurs at $\Gamma \sim \sqrt{\tau}$ and τ might be fixed by a threshold requirement. Nevertheless, it would be too long to treat here the choice of the x-ray detector, of the foil material, of the gas, and of the repartition of foils and detectors. This deserves a further publication.

Computational prescriptions

To get the predicted $W_{\rm det}$, we have to calculate $G_{\rm many}(\nu, \Gamma, \tau)$ or $G_{\rm many}(\nu', \Gamma', \tau')$ for several values of ν and Γ. We rewrite it as $F(a, V, \tau)$, with a and V given by (3.26) and (3.28). F is given by (3.67) or (3.69). For large τ, it is clear that the number of δ functions to sum over is very big and that the single-foil formula is valid, except for the contributions of the lowest integers p. Besides, when y is very large, the $\sin^2$ factor can be replaced by $\frac{1}{2}$, i.e., we can use the single-surface integrand. Therefore we must divide the semistraight line Px (or the $y>0$, $\varphi_2>0$ quadrant) in three regions:

a "δ" region, let us say $\varphi_2 \leq 4\pi$, where (3.69) must be integrated exactly;

a "single-foil" region, $\varphi_2 > 4\pi$, $y \leq y_{\rm inco}$, where we use (3.67) without the N-foil interference factor $2\pi \sum_p \delta(\cdots)$. $y_{\rm inco}$ must be such that the $\sin^2$ factor is maximum or minimum, for instance,

$$y_{\rm inco} + V = 2\pi \ \text{integer}(3 + V/2\pi) . \tag{4.38}$$

To integrate the $y \sim 2a$ peak correctly, it is sufficient to take the integration points y_i in a geometrical progression, such that $\Delta y_i \sim 1$ near $y \sim y_{\rm inco}$;

an "incoherent" region, where all interference factors are neglected in (3.67), and whose contribution can be calculated analytically.

The regions are shown in Fig. 13. The precision obtained is expected to be 5 or 10%, and can be improved by increasing $y_{\rm inco}$ and enlarging the δ region.

A big economy of computing time can be made in the case where we have to calculate G for many values of Γ (for instance, when we want to draw a curve versus Γ). We split $F(a, V, \tau)$ in two functions

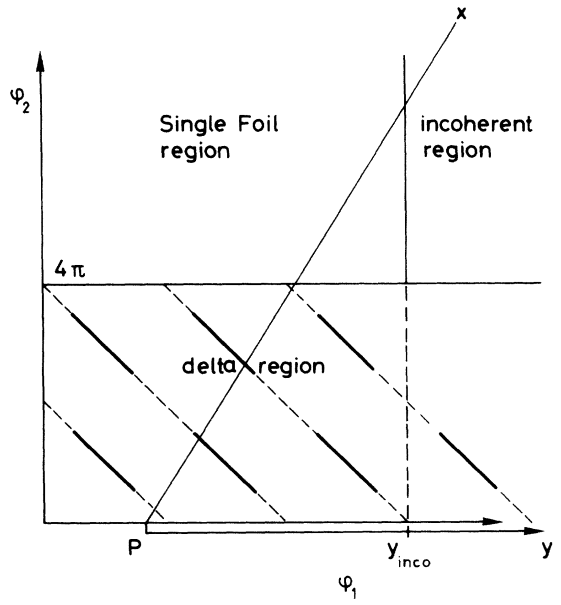

FIG. 13. The different domains where one can neglect one, two, or no interference factor in (3.69).

$$F = F_1 - aF_2 , \tag{4.39}$$

$$F_{1,2} = V^2 \int_a^\infty y^{-1,-2}(y+V)^{-2} dy \times (\text{interference factors}) . \tag{4.40}$$

When changing Γ ($\Gamma_m \to \Gamma_{m+1} > \Gamma_m$), we need only to integrate (4.40) between a_{m+1} and a_m, instead of a_{m+1} and infinity.

ACKNOWLEDGMENTS

One of us (X.A.) wishes to thank the Aspen Center for Physics, where part of this work has been done, and C. W. Fabjan for discussions.

*Work supported in part by the National Science Foundation.

†Laboratory associated with CNRS.

[1]V. L. Ginzburg and I. M. Frank, Zh. Eksp. Teor. Fiz. 16, 15 (1946).

[2]For extensive reviews, see for instance the following: a. G. M. Garibyan, Yerevan report EØ-27, 1973 (unpublished); b. M. L. Ter Mikaelyan, Nucl. Phys. 24, 43 (1961); c. M. L. Ter Mikaelyan, *High Energy Electromagnetic Processes in Condensed Media* (Wiley-Interscience, New York, 1972); d. F. G. Bass and V. M. Yakovenko, Usp. Fiz. Nauk 86, 189 (1965) [Sov. Phys.—Usp. 8, 420 (1965)].

[3]A paper in the same spirit has been written recently by Loyal Durand III, Phys. Rev. D 11, 89 (1975).

[4]See also M. L. Cherry, G. Hartmann, D. Müller, and T. A. Prince, Phys. Rev. D 10, 3594 (1974).

[5]G. M. Garibyan, *Adventures in Experimental Physics* (World Science Education, Princeton, 1972), p.120.

[6]In this paper we take units such that $\hbar = c = 1$. We shall often use the relation eV × micron = 5.

[7]G. M. Garibyan, Zh. Eksp. Teor. Fiz. 37, 527 (1959) [Sov. Phys.—JETP 10, 372 (1960)].

[8]L. C. L. Yuan, C. L. Wang, H. Uto, and S. Prünster, Phys. Rev. Lett. 25, 1513 (1970).

[9]We disagree with the formula $y_s \sim \omega_{P_t} l_2/4\pi$ of Ref. 4 (our y_s is lower).

[10]R. Ellsworth, J. MacFall, G. Yodh, F. Harris, T. Katsura, S. Parker, V. Peterson, L. Shiraishi, V. Stenger, J. Mulvey, B. Brooks, and J. Cobb, in *Proceedings of the Thirteenth International Conference on Cosmic Rays, Denver, 1973* (Colorado Associated U. P., Boulder, 1973) Vol. IV, p. 2819.

[11]The stationary thresholds are, in fact, those mentioned in Refs. 2b [Eq. (2.10)], 2c [Eq. (28.90)], and 2d [Eq. (6.19)]. They have recently been observed [C. W. Fabjan and W. Struczinski, Phys. Lett. 57B, 483 (1975)].

[12]See, for instance, B. Rossi, *High Energy Particles* (Prentice Hall, New York, 1952).

[13]The coefficient 0.75 has been obtained by fitting numerical results of H. S. Snyder and W. T. Scott, Phys. Rev. 76, 220 (1949), shown in Fig. 3 of their paper. They give the probability distribution for the projected angle β_x or β_y, and we assume $\tilde{\beta} \simeq \sqrt{3}\beta_x$, which is true for most bell-shaped distributions.

[14]G. M. Garibyan and I. Ya. Pomeranchuk, Zh. Eksp. Teor. Fiz. 37, 1828 (1959); G. M. Garibyan, Zh. Eksp. Teor. Fiz. 39, 332 (1960) [Sov. Phys.—JETP 12, 237 (1961)].

[15]V. E. Pafomov, Zh. Eksp. Teor. Fiz. 47, 530 (1964) [Sov. Phys.—JETP 20, 353 (1965)]. Dokl, Akad. Nauk SSSR 133, 1315 (1960) [Sov. Phys.—Dokl. 5, 850 (1960)].

[16]I. I. Goldman, Zh. Eksp. Teor. Fiz. 38, 1866 (1960) [Sov. Phys.—JETP 11, 1341 (1960)].